



HAL
open science

Optical Analysis of p-Type Surface Conductivity in Diamond with Slotted Photonic Crystals

Candice Blin, Xavier Checoury, Hugues Girard, Celine Gesset, Samuel Saada,
Philippe Boucaud, Philippe Bergonzo

► **To cite this version:**

Candice Blin, Xavier Checoury, Hugues Girard, Celine Gesset, Samuel Saada, et al.. Optical Analysis of p-Type Surface Conductivity in Diamond with Slotted Photonic Crystals. *Advanced Optical Materials*, 2013, 1, pp.963 - 970. 10.1002/adom.201300331 . cea-01791383

HAL Id: cea-01791383

<https://cea.hal.science/cea-01791383>

Submitted on 11 Feb 2019

HAL is a multi-disciplinary open access archive for the deposit and dissemination of scientific research documents, whether they are published or not. The documents may come from teaching and research institutions in France or abroad, or from public or private research centers.

L'archive ouverte pluridisciplinaire **HAL**, est destinée au dépôt et à la diffusion de documents scientifiques de niveau recherche, publiés ou non, émanant des établissements d'enseignement et de recherche français ou étrangers, des laboratoires publics ou privés.

Advanced Optical Materials

Optical Analysis of p-Type Surface Conductivity in Diamond with Slotted Photonic Crystals

--Manuscript Draft--

Manuscript Number:	adom.201300331R1
Full Title:	Optical Analysis of p-Type Surface Conductivity in Diamond with Slotted Photonic Crystals
Article Type:	Full Paper
Keywords:	CVD nanocrystalline diamond; photonic crystals; Nanocavities; Surface conductive layer; Transfer doping.
Corresponding Author:	Candice Blin Diamond Sensors Laboratory Gif sur Yvette, FRANCE
Corresponding Author Secondary Information:	
Corresponding Author's Institution:	Diamond Sensors Laboratory
Corresponding Author's Secondary Institution:	
First Author:	Candice Blin
First Author Secondary Information:	
Order of Authors:	Candice Blin
	Xavier CHECOURY
	Hugues GIRARD
	Céline GESSET
	Samuel SAADA
	Philippe BOUCAUD
	Philippe BERGONZO
Order of Authors Secondary Information:	
Abstract:	<p>We report on the fabrication of two-dimensional slotted diamond-based photonic crystals (PhC) with Q factors up to 6500 and their optical characterization at 1550 nm in order to probe surface molecular modifications. In this study, we intentionally focus on the simplest surface modifications that can modify the diamond PhC optical properties, namely, hydrogenation and oxidation. We observed that, depending on the chemical surface termination, these diamond PhCs exhibit a strong modification of their spectral features. When the surface is tuned from oxidized to hydrogenated, a resonance wavelength shift of the cavity occurs and is accompanied by a decrease of the Q factor. Moreover, we give experimental evidence that this phenomenon is reversible as the initial value of the Q factor is recovered when the surface is re-oxidized. We attribute this result to the sub-surface conductive layer that is due to transfer doping in hydrogenated diamond and which is absent from oxidized diamond. Thanks to 3D-FDTD simulations, we give an estimate of the effective refractive index of the surface conductive layer at 1.5 μm as a function of its thickness. This result highlights the high sensitivity of slotted diamond PhC and the importance of surface control for biosensing with diamond.</p>
Additional Information:	
Question	Response
Please submit a plain text version of your cover letter here.	Response for manuscript adom.201300331 "Optical Analysis of p-Type Surface Conductivity in Diamond with Slotted Photonic Crystals" Dear Dr Fuchs, We have

<p>Please note, if you are submitting a revision of your manuscript, there is an opportunity for you to provide your responses to the reviewers later; please do not add them to the cover letter.</p>	<p>uploaded a revised manuscript referenced adom.201300331 entitled "Optical Analysis of p-Type Surface Conductivity in Diamond with Slotted Photonic Crystals". We thank the reviewers for their positive remarks as well as their helpful comments for improving the manuscript. All the comments of the reviewers have been answered. This letter includes the revised version of the manuscript with the main modifications emphasized in red color. Considering the improvements brought to the delivered manuscript, we hope that this revised version is now suitable for publication in Advanced Optical Materials. Sincerely yours, Candice Blin</p>
--	---

DOI: 10.1002/adom.201300331

Full paper

Title : Optical Analysis of p-Type Surface Conductivity in Diamond with Slotted Photonic Crystals

*Authors : Candice Blin, Xavier Checoury *, Hugues Girard, Céline Gesset, Samuel Saada, Philippe Boucaud and Philippe Bergonzo **

C. Blin, Dr. H. Girard, C. Gesset, Dr. S. Saada, Dr. P. Bergonzo
CEA, LIST, Diamond Sensors Laboratory, Gif-sur-Yvette, F-91191, France
E-mail : philippe.bergonzo@cea.fr

C. Blin, Prof. X. Checoury, Dr. P. Boucaud
IEF, CNRS Univ Paris Sud 11, Bâtiment 220, F-91405 Orsay Cedex, France
E-mail : xavier.checoury@ief.u-psud.fr

Keywords: CVD nanocrystalline diamond, Photonic crystals, Nanocavities, Surface conductive layer, Transfer doping

We report on the fabrication of two-dimensional slotted diamond-based photonic crystals (PhC) with Q factors up to 6500 and their optical characterization at 1550 nm in order to probe surface molecular modifications. In this study, we intentionally focus on the simplest surface modifications that can modify the diamond PhC optical properties, namely, hydrogenation and oxidation. We observed that, depending on the chemical surface termination, these diamond PhCs exhibit a strong modification of their spectral features. When the surface is tuned from oxidized to hydrogenated, a resonance wavelength shift of the cavity occurs and is accompanied by a decrease of the Q factor. Moreover, we give experimental evidence that this phenomenon is reversible as the initial value of the Q factor is recovered when the surface is re-oxidized. We attribute this result to the sub-surface conductive layer that is due to transfer doping in hydrogenated diamond and which is absent from oxidized diamond. Thanks to 3D-FDTD simulations, we give an estimate of the effective refractive index of the surface conductive layer at 1.5 μm as a function of its thickness. This result highlights

1 the high sensitivity of slotted diamond PhC and the importance of surface control for biosensing
2 with diamond.
3
4
5
6

7 **1. Introduction**

8
9 Using integrated photonic technologies, it is possible to fabricate very compact, high performing
10 and low-cost chemical and biochemical sensors. Different kinds of integrated optical chemical
11 sensors have been proposed over the years, from those based on surface plasmon resonance ^[1] to
12 micro-ring resonators.^[2] A novel class of nanoscale biosensors which have been increasingly
13 studied in recent years is photonic crystals (PhCs). Such devices can offer unique and high
14 sensitivity for the detection of specific chemical and biological agents using small active volumes,
15 thus making them promising structures for their use in medical or environmental applications. PhCs
16 generally consist of a one- or two-dimensional periodically patterned dielectric structures where
17 light can be confined to in-plane guided resonance modes in the slab. They are characterized by
18 spectral features such as the resonance wavelength or the quality factor (Q). Most of the recent
19 designs for cavities with high quality factors rely on the creation of an optical confinement along a
20 W1 waveguide (one missing line of holes in a triangular lattice PhC). This can be achieved for
21 instance by a variation of the lattice constant ^[3] or of the width of the waveguide.^[4]
22
23
24
25
26
27
28
29
30
31
32
33
34
35
36
37
38
39
40

41 Due to the tight confinement of the optical mode, PhCs are highly sensitive to local changes in their
42 environment, ^[5] such as the refractive index, which affect the resonance wavelength and the quality
43 factor of the resonator. This shift of the resonance wavelength thus confers a sensing capacity to the
44 cavity. Specificity in detection is brought by functionalizing the surface of the resonant cavity or
45 waveguide, which can then be used to selectively capture a specific target molecule, in gas or liquid
46 phase.^[6,7] The detection limit will thus be linked to the quality factor of the cavity, and so
47 challenging Q factors are needed to obtain sufficiently sensitive sensors.
48
49
50
51
52
53
54
55
56
57

58 Nowadays, silicon is the reference material for such devices thanks to its optical properties and its
59 well mastered nanostructuration. Recently, quality factor of a few tens of thousands were obtained
60
61
62
63
64
65

1 in silicon PhC sensor cavities allowing to detect ultra-small refractive index changes at the surface
 2 of the sensors corresponding to an avidin bounded mass of approximately 100 ag.^[6] However, it has
 3
 4
 5 been reported that the quality factor of micro-disk resonators may vary from a factor of one to five
 6
 7 when the silicon surface is changed from oxide to hydrogenated termination.^[8] This strong
 8
 9 dependence was pointed out as one of the most critical challenge for future Si micro- and
 10
 11 nanophotonic systems where extremely high Q-factors are usually required. Furthermore, PhC
 12
 13 sensing devices will require a highly stable material to avoid any unsolicited perturbation of the
 14
 15 surface, and surface stability of silicon may be a limitation, especially its functionalization which
 16
 17 may display unstable properties in biological media.^[9]

21
 22 Among the dielectric materials available for PhC fabrication, diamond appears as a promising
 23
 24 alternative to build such photonic-based devices: it is recognized to be an outstanding material in
 25
 26 terms of mechanical properties, as well as in terms of bio-compatibility and surface
 27
 28 functionalization. Diamond-based devices are now at an advanced state of development in the fields
 29
 30 of electrochemistry, MEMS sensors, biomedical implants, protective coatings, *etc.*^[10] Diamond is
 31
 32 currently emerging as a novel material for the development of photonics devices at a micrometric
 33
 34 scale.^[11] It exhibits a refractive index of 2.4, and diamond wide band gap offers transparency in a
 35
 36 large spectral range from ultraviolet to far infrared spectral bands unlike Si which, in particular, is
 37
 38 not transparent in the visible range. Indeed, these properties have already allowed the recent
 39
 40 fabrication of photonic crystal cavities with quality factors reaching 3000, not only on 3x3 mm²
 41
 42 monocrystalline substrates,^[12,13] but also on polycrystalline diamond layers^[14] grown on two inches
 43
 44 substrates, thus opening the route to large scale processing with standard nanotechnology
 45
 46 techniques. Further, since diamond, unlike Si, does not have a native oxide, it exhibits a stable
 47
 48 surface which can be functionalized through a covalent carbon-carbon binding,^[15] highly promising
 49
 50 towards the fabrication of diamond-based photonic devices for chemical detection.

51
 52 In this context, this work aims at evaluating how surface chemistry affects the optical properties of
 53
 54 diamond-based photonic devices. If sophisticated and stable functionalizations are allowed on
 55
 56
 57
 58
 59
 60
 61
 62
 63
 64
 65

1 diamond surfaces, they rely on the stability of the initial surface terminations, usually either
2 “hydrogenated” with C-H bonds, or “oxidized” with etheric, alcohol or carboxylic groups. These
3 terminations are the prerequisite to any further functionalization, opening the route to specific
4 grafting routes such a diazonium salts chemistry, peptidic linking, *etc.* Therefore, the effect of this
5 basic surface chemistry on diamond optical properties has been studied in this work by the means of
6 a specifically designed PhC. We use a slotted photonic crystal (sPhC) cavity to get a high sensitivity
7 to surface refractive index change and then tune the diamond surface termination between
8 hydrogenated and oxidized. As will be shown, a wavelength shift of the cavity occurs and is
9 accompanied by a decrease of the Q factor when the surface chemistry is simply turned from
10 oxidized to hydrogenated. This effect is reversible. These phenomena are attributed to the
11 conductive layer known to exist from transfer doping on hydrogenated diamond surfaces, and we
12 will below demonstrate how this feature will correlate with the behavior of such diamond-based
13 photonic devices.
14
15
16
17
18
19
20
21
22
23
24
25
26
27
28
29
30

31 **2. Results and discussion**

32 **2.1. Simulation of slotted photonic crystals cavities**

33
34 A few types of PhC cavities have already been simulated and measured on diamond.^[16] The so
35 called L3 or L7 cavities^[12,17] can present modes with quality factors up to a few thousands while
36 modulated-width type cavities^[14] can theoretically reach Q factors above 1 million. So far there is
37 no simulation result on slotted microcavities on diamond and only a few simulations have been
38 reported on long slotted waveguides.^[18] The parameters that lead to the highest Q factors and
39 smallest modal volumes for these slotted cavities may be different from the ones made in silicon
40 due to the lower refractive index of diamond. In the following section, the best parameters to
41 achieve high Q factors and small modal volumes are determined by using three dimensional finite
42 differences in time domain simulations (3D-FDTD). The cavity design is similar to the one
43 fabricated on silicon and described in ref.^[19]. This design consists of a modulated width cavity
44
45
46
47
48
49
50
51
52
53
54
55
56
57
58
59
60
61
62
63
64
65

similar to ref.^[3] with a slot (See **Figure 1.a.**) and is thus different from the designs proposed in ref.^[20]. The parameters that can be varied to optimize the performance of the cavity are the slab thickness, h , the slot width, l , the waveguide width W , the radius of the air holes, r , and the hole displacement d . The lattice constant of the PhC, a , is set to 620 nm and can be adjusted so that the cavity resonance precisely meets the target wavelength since all the photonic crystal parameters can be rescaled. To ensure single-mode operation at wavelengths near $\lambda=1600$ nm, a slab thickness h of 360nm is chosen. A slot width of 135 nm allows a high confinement of the light in the slot while being easily fabricated. Indeed, narrower 75 nm-wide slots have also been simulated and give similar results in terms of quality factor and modal volume. As in silicon,^[19] the best Q factors are achieved with waveguides larger than the standard W1 waveguide, that is made by removing one row of holes from a perfect photonic crystal. The width of the studied waveguide is $1.15\sqrt{3}a$, *i.e.* 1.15 times the width of a W1 waveguide. This comes from the necessity to keep the resonating mode in the center of the photonic band gap to get a good lateral confinement and a good quality factor by keeping a theoretical mode well below the light cone. For this set of parameters, we study the quality factor and the modal volume V as a function of the holes radius of the PhC and of the hole displacement d that define the cavity. As can be seen on **Figure 1.b.** that displays the evolution of the quality factor for different hole radius and displacement d , a theoretical Q factor up to 0.8×10^6 can be expected from these cavities on diamond, a value that is comparable to those reported on silicon. The modal volumes, represented in **Figure 1.c.**, are of the order of $0.15 \lambda_0^3$ with λ_0 the wavelength in vacuum. This value is two to three times larger than the one achieved in silicon for the same slot widths because of the smaller index contrast and of the resulting lower confinement in diamond *vs.* silicon. Nevertheless, for a typical period of 620 nm, the corresponding sensing volume gets down to a value of 650 attoliter, an extremely small value achieved thanks to the high confinement properties of PhCs.

The mode pattern calculated with a 3D-FDTD simulation of the slotted PhC cavity is shown in **Figure 1.d.** It illustrates that the mode profile is well confined in the low refractive index medium,

thus ensuring an optimized sensitivity to any refractive index change in the slot as well as to any surface modification of the PhC slot. Generally, a measure of the resonant wavelength shift versus the change of the refractive index is the appropriate measure for defining the sensitivity of the optically resonant refractive index sensor.^[21] For example, simulations show a change of the resonance wavelength of 580 pm for a refractive index change of the PhC environment of 10^{-3} , i.e. a sensitivity of 580 nm by refractive index unit (RIU). The detection limit of this kind of sensors depends on its capability to accurately measure the spectral shift which in turns depends on the Q factor of the cavity but also on the experimental setup. Following the approach of ref.^[21], a rough estimate of the detection limit based on our experimental conditions is 3×10^{-6} RIU.

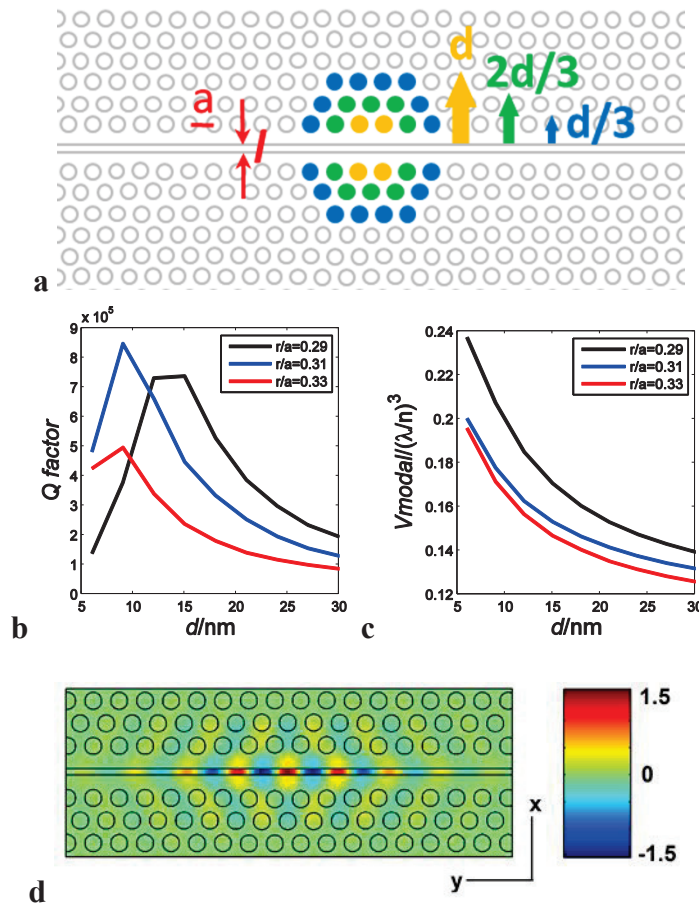


Figure 1. a) Schematic representation of the photonic crystal design with a modulated width cavity and three different hole displacements, a slot width l and a period a . b) Simulated Q factors (3D-FDTD) of the cavities as a function of hole displacements d for different normalized radii r/a . c) Simulated modal volumes of the cavities in units of $(\lambda/n)^3$, with $n=1$ (air), as a function of hole displacements d for different normalized radii r/a . d) Simulation of slotted photonic crystal air

cavity showing E_y component of mode profile at cavity resonant wavelength $\lambda=1550\text{nm}$, arbitrary unit.

2.2. Fabrication and optical characterization of the PhCs

Slotted nanocrystalline diamond PhCs on an integrated photonic platform were fabricated according to the previously described structures (see experimental section for details). **Figure 2** shows scanning electronic microscope (SEM) views of the sPhC at the end of the process.

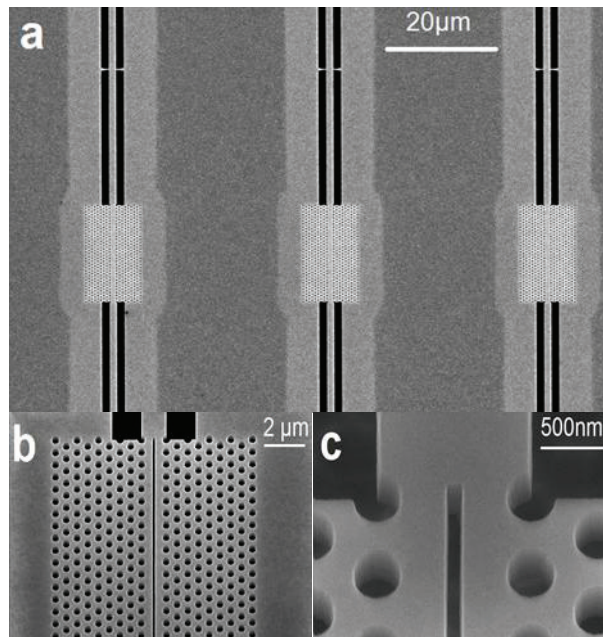


Figure 2. Scanning electron microscope (SEM) views of the fabricated slotted photonic crystal in polycrystalline diamond. **a)** SEM view of three photonic crystal cavities with their access waveguides maintained by nanotethers. **b)** Tilted view (45°) of a PhC and its access waveguide with the slot at the center. **c)** Tilted close view of a PhC with the 135-nm wide slot and its access waveguide.

Figure 2.a. is a top view of three sPhCs displaying their access waveguide maintained by nanotethers. These 250- μm long waveguides are terminated by inverted tapers (not shown here) that allow an efficient in-plane light injection from a microscope objective or an optical fiber.^[14,22] The magnification (tilted view at 45°) shown in **Figure 2.b.** and **2.c.** reveals slightly tilted air holes sidewalls relatively to the vertical direction. The verticality of holes is estimated to be better than 3° , indicating a good quality of the diamond etching process that is enough to reach very high Q factors

since it has been shown that such an angle theoretically allows for quality factors up to 3×10^6 in silicon PhC cavities.^[23]

Figure 3 presents an example of the experimental transmission of a PhC with a period $a=630$ nm and a slot width of 75 nm.

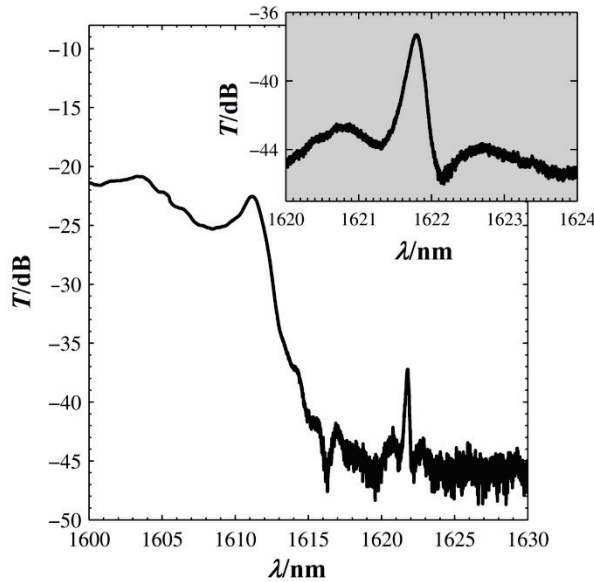
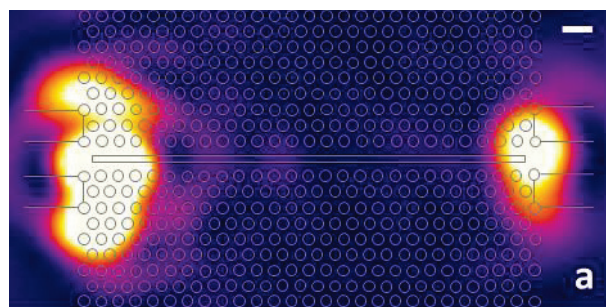


Figure 3. Fiber-to-fiber transmission (T) spectrum of a slotted PhC with a Q factor of 6500. Inset: zoom on the resonance.

The photonic crystal acts as a waveguide for wavelengths shorter than 1615 nm, as confirmed from the observation of the emitted light from the surface, here observed using an infrared camera on **Figure 4.a.**, and a fiber-to-fiber transmission mean value of -23 dB is measured. The TE photonic band gap in the diamond PhC waveguide is seen for wavelengths longer than 1622 nm where the transmission remains below -45 dB. The corresponding optical image at this wavelength is shown on **Figure 4.b.** Finally, the transmission peak at 1621.8 nm is clearly associated with the cavity mode as presented on **Figure 4.c.**



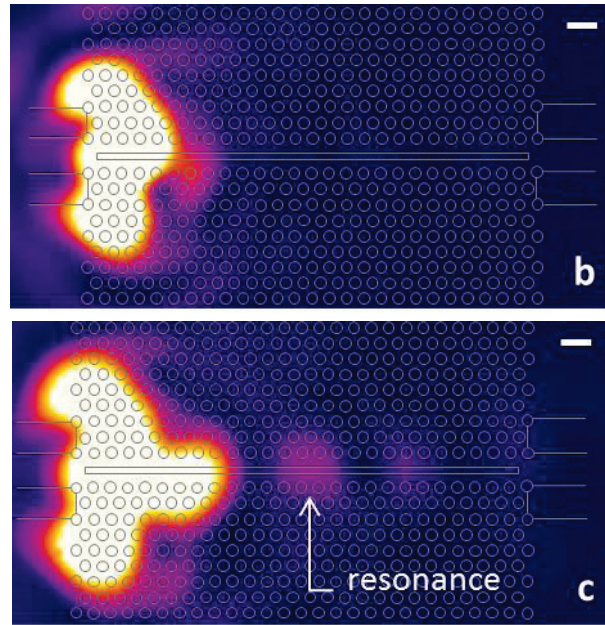


Figure 4. Optical images of the cavity at different wavelengths in false colors. For clarity, a schematic representation of the PhC is superimposed. **a)** waveguide transmission. **b)** cut off in the photonic band gap. **c)** cavity mode resonating at 1621.8 nm. Scale bar : 1 μm .

The measured quality factor for this sPhC reaches 6500. Regarding other diamond-based photonic devices, the value measured here for our polycrystalline diamond-based PhC is one among the highest Q factors reported in the literature,^[13,24] and can be even compared with PhCs processed from high quality monocrystalline diamond.^[12,25] The discrepancy of several orders of magnitude between the simulated value and the experimental Q factor is usual in silicon and is generally attributed to fabrication imperfections and surface roughness. Light scattering at grain boundaries in polycrystalline diamond is another source of losses that occurs here and does not exist in silicon PhCs nor in the PhCs made in mono-crystalline diamond. **Future work on polycrystalline diamond with different grain size will clearly identify the quantitative impact of scattering on Q factors.** Nevertheless, the Q factor achieved is only twice lower than those achieved in silicon for similar designs of slotted cavities.^[26] Compared to the diamond PhC cavities we reported in previous works,^[14] the introduction of a slot at the center did not affect the Q factor of the cavity significantly. The quality of the structure has even been significantly optimized, mainly through the use of a nitride mask instead of a silica one resulting in a better quality etching (see methods). These Q

1 factor values are of the same order as those used on silicon to realize molecular detection at the PhC
2 surface.^[6]
3
4
5
6

7 **2.3. Characterization of the chemical modifications**

8
9 As described above, the slotted polycrystalline diamond-based PhC exhibits a Q factor and a design
10 which are both well adapted to probe the effect of a chemical surface modification. A diamond
11 surface is known to be a versatile platform toward functionalization, thanks to its carbon-related
12 chemistry. In this study, we intentionally focus on the simplest surface modifications to probe the
13 sensitivity of the diamond slotted PhC cavity and the effects of these surface terminations on the
14 PhC optical properties. Hydrogenated and oxidized terminations are also the base of the most
15 common surface functionalization performed on diamond-based devices. For instance, biological
16 moieties such as nucleic acids or proteins can covalently be grafted by their amino groups onto
17 diamond devices, either through an amidation process starting from carboxylic groups ^[27] or
18 through the direct amine grafting onto an hydrogenated surface.^[28] Such surface terminations can be
19 easily conferred to diamond by physico-chemical treatments, such as plasma treatments, annealing
20 or photochemistry. Here we have explored the effect of two surface terminations, based on (i) a
21 plasma hydrogenation of the sample, to saturate homogeneously the diamond surface with C-H
22 terminations,^[29] and (ii) an oxidation step under UV/Ozone.^[30]
23
24
25
26
27
28
29
30
31
32
33
34
35
36
37
38
39
40
41
42
43

44 After each surface treatment, XPS analysis were carried out to investigate the surface modifications
45 induced by the hydrogenation and oxidation treatments. XPS general survey of the hydrogenated
46 diamond reveals that only a small amount (1.4 at.%) of oxygen remains on the surface, which is
47 partly due to a surface contamination during the transfer between the CVD reactor and the XPS
48 chamber. Note that traces of fluorine are also detected (0.35 at.%) and can be attributed to a
49 contamination during the fabrication process of PhC as several fluorine-based process are used.
50
51 After UV/Ozone oxidation, the oxygen quantity increases up to 10.6 at.%, thus confirming an
52 efficient oxidation of the surface.
53
54
55
56
57
58
59
60
61
62
63
64
65

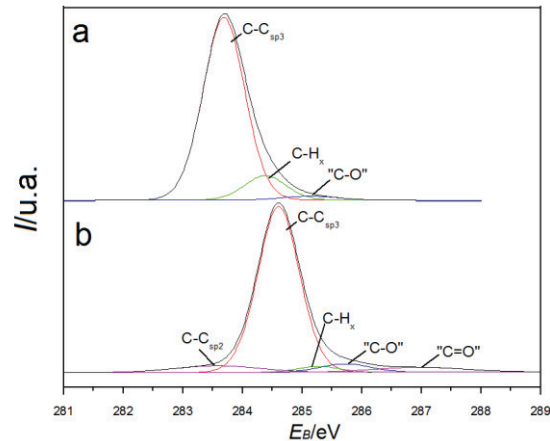


Figure 5. C1s core level spectra of a) hydrogenated and b) oxidized diamond layers

Figure 5.a. and b. report the fitted C1s core level spectra of the diamond layers after hydrogenation and oxidation treatments respectively. On the hydrogenated sample, the main component attributed to the C-C sp³ diamond bonds is located at 284 eV. For an undoped material, this value is a little bit lower than expected, and can be attributed to the superficial conductive layer, which induces a surface band bending, revealed by a downshift on the C1s XPS spectrum, as already evidenced by several authors in the literature.^[31,32] Two others components were identified, attributed to CH_x and etheric bridges, located at +0.7 and +1.5 eV from the C-C sp³ peak, respectively.^[33] The component related to the carbon-oxygen groups represent ca. 2% of the C1s core level, which is in agreement with the 1.4 at.% of oxygen detected on the sample. After oxidation, a strong modification of the C1s core level occurs. First, a strong upshift is observed, with the main component attributed to the C-C sp³ diamond bonds located at 284.9 eV, *i.e.* +0.9 eV *vs.* the hydrogenated sample. This shift towards higher binding energies of the C1s peak can be related to the loss of the surface conductive layer after the removal of the hydrogenated terminations. This effect has already been evidenced by Ballutaud *et al.* on equivalent nanocrystalline materials.^[32] The proportion of the component related to the etheric bridges increases up to 5% of the C1s core level, while a new component located at +2.4 eV is identified, attributed to carbonyl functions, and also representing 5% of the C1s core level. At -1 eV, a shoulder is observed, due to the presence of C-C sp² for 5%. A slight surface

graphitization of the sample seems to occur during the UV/Ozone oxidation, which explains the appearance of this new component.

2.4. Optical characterization of the modified sPhC

Prior to any surface modification, measurement of a slotted photonic crystal transmission spectrum just after the end of the process was recorded as a reference. We measured PhC cavities with a period $a=630$ nm, and the structures exhibit a 9-nm shift of the central holes.

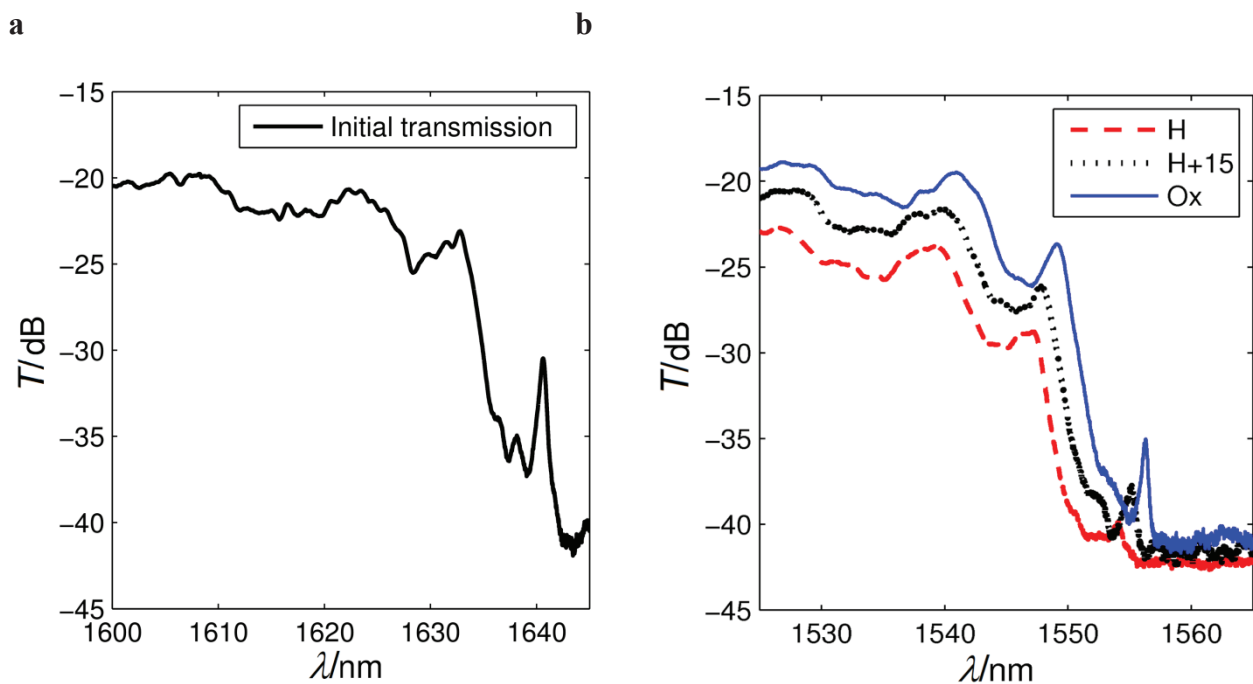


Figure 6. Transmission spectra of the photonic crystal cavities for different surface states. **a)** Spectrum at the end of the process. **b)** (dash red) hydrogenated PhC – (dot black) hydrogenated PhC after 15 days – (blue) oxidized PhC

Parameters: $a=630$ nm, $r=0.31a$, slot=135nm, barrier length=8, $d=9$ nm

The transmission spectrum is presented on **Figure 6.a**. A Q factor of 2000 was measured with a peak resonance at 1640.8 nm. Indeed, we chose a PhC cavity with a shorter barrier in order to have better transmission for the experimental measurements. The coupling coefficient between the access waveguide and the cavity is consequently different and this is why the Q factor is lower (see methods). However, this value remains perfectly adapted for the chemical study as will be shown.

We then compared the resonance wavelength and quality factors of the same cavity after different

1 successive surface treatments, namely hydrogenation and then oxidation. **Figure 6.b.** shows the
 2 transmission spectra of the same diamond slotted cavity for different surface chemical states. The
 3 black curve corresponds to a freshly hydrogenated photonic crystal cavity. As a first observation, we
 4 see that the peak resonance is strongly downshifted from 1640.8 to 1554.1 nm and the Q factor also
 5 decreased to 650, which is three times below the initial value. The downshift of the peak resonance
 6 can be attributed to a 6-nm etching occurring during the hydrogenation step, which was confirmed
 7 by ellipsometry. Such etching of the surface is inherent to the plasma hydrogenation treatment, but,
 8 as shown by the XPS analysis, does not affect the quality of the diamond surface. However,
 9 according to the simulations, the Q-factor decrease cannot only be attributed to diamond etching.
 10 After ageing for 15 days in air, transmission of the same sample was recorded again and is
 11 represented by the red curve on Figure 6.b. Surprisingly, the resonance peak of the PhC cavity
 12 presents a red shift of 1.1 nm (1555.2 nm) while the Q factor increases to reach a value of 1050.
 13 Finally, when an intentional surface oxidation is performed on the sample, through the UV/ozone
 14 treatment, the red shift continues to occur, with a shift of +1.1 nm (1556.3 nm) and a value of the Q
 15 factor back to the initial one, namely 2000. The transmission also evolves according to the surface
 16 modification. An increase is observed when the sample changes from a hydrogenated state to an
 17 oxidized one. It is particularly observable in the allowed transmission frequency range for
 18 wavelengths shorter than 1550 nm and at the cavity resonance frequency.

2.5. Effect of the chemical modification on PhC optical properties

29 From these experiments, our polycrystalline diamond-based PhCs clearly exhibit a strong
 30 dependence on the surface state, with a high sensitivity to the nature of the surface terminations
 31 revealed by both resonance peak position and value of the Q factor. Since the refractive index
 32 change at the diamond surface is expected to be very small, the evolution of the resonant frequency
 33 and quality factor can be estimated thanks to first order perturbations. Indeed, the shift $\Delta\omega$ of the
 34 resonant frequency of a cavity due to a small change $\Delta\varepsilon$ of the dielectric constant $\varepsilon(\vec{r})=n^2(\vec{r})$, with

n the refractive index of the materials making up the cavity, is given with a second order accuracy by **Equation (1)** :

$$\Delta\omega = \frac{\omega}{2} \frac{\iiint \Delta \varepsilon(\vec{r}) \|\vec{E}(\vec{r})\|^2 d^3\vec{r}}{\iiint \varepsilon(\vec{r}) \|\vec{E}(\vec{r})\|^2 d^3\vec{r}} + O((\Delta\varepsilon)^2) \quad (1)$$

where $\vec{E}(\vec{r})$ is the electric field of the unperturbed resonant mode.^[34] A small absorption, represented by the imaginary part of the refractive index or the dielectric constant, leads to a complex frequency shift. The imaginary part of this shift represents a cavity field decreasing as $e^{-Im(\Delta\omega t)}$ or in other words a cavity mode with a quality factor of $Q_a = \frac{\omega}{2Im(\Delta\omega)}$. The total quality factor Q_t of the cavity is then given by **Equation (2)**:

$$Q_t^{-1} = Q_u^{-1} + Q_a^{-1} \quad (2)$$

where Q_u is the quality factor of the unperturbed cavity.

Here, the $\vec{E}(\vec{r})$ field of the unperturbed cavity resonant mode has been calculated by 3D-FDTD once and the perturbative approach has been used to calculate the frequency shifts much faster than with a full 3D calculation. However, a few supplementary FDTD calculations have been performed to check that this perturbative approach is accurate enough to explain the experimental results. Considering that when the surface is tuned from hydrogenated to oxidized the chemical modification is of the order of the molecule layer, the refractive index modification at the surface should be effective over a thickness of the order of a few Angstroms, as can be expected with the progressive replacement of a H termination by a O termination. However, the expected very small refractive index change resulting from such replacement is not compatible with the frequency shifts observed with the recorded values beyond 2 nm. Obviously, we can also consider that adsorbed molecules or groups of adsorbates, with a thickness of several nm, can be deposited at the surface. Then the frequency shift can reach the 2 nm observed. However, if such an hypothesis turned out to be true, then the Q factor would not increase as observed, because these adsorbates cannot bring

1 optical gain. Actually, the initial value is recovered, which means that there is an intern
2 phenomenon related to the properties of the layer and that it is not just a chemical effect.
3

4
5 To explain this phenomenon, we have to get back to the transfer doping model.^[35] It is well known
6 that hydrogenated terminations confer to diamond films specific electronic properties.^[36] Diamond
7 surface becomes conductive when hydrogenated. The creation of a surface conductive layer (SCL)
8 due to *transfer doping* has already been thoroughly described in the literature, and is known to
9 disappear when the surface is oxidized. Maier and coworkers presented about a decade ago the
10 associated mechanism.^[35] The extension of this conductive layer is usually considered to be
11 between 5 and 30 nm from the diamond surface.^[37] Such a layer may affect the optical properties of
12 the diamond surface though it has never been characterized so far. Indeed, the absorption
13 phenomenon inherent to such conductive materials would be consistent with the experimental
14 evolution of our quality factor. When the surface is freshly hydrogenated, the surface conductivity is
15 high as well as the loss and the imaginary part of the refractive index. The surface loses partly its
16 conductivity when aged in air,^[38] as hydrogenated diamond surfaces are known to be sensitive to air
17 exposure, with a limited but effective spontaneous surface oxidation, with the creation of oxidized
18 terminations among the hydrogenated ones.^[39] Then, the conductivity completely drops down when
19 the surface is oxidized by UV/O₃ treatment, which induces the fall of the imaginary part of the
20 refractive index. Note that the rise of the transmission is also consistent with the continuously
21 disappearing surface conductivity since the losses due to the propagation along the hydrogenated
22 access waveguides and PhC structure decrease. The transmission of the PhC at the resonance
23 frequency can also be attributed to the cavity losses but the transmission measurement of the PhC,
24 as opposed to the quality factor measurement, is affected by uncertainties such as the evolution of
25 the coupling efficiency and access waveguide transmission in hydrogenated diamond.
26
27
28
29
30
31
32
33
34
35
36
37
38
39
40
41
42
43
44
45
46
47
48
49
50
51
52
53
54

55 For a given thickness of the surface conductive layer, we can relate the resonant wavelength shift
56 and the evolution of the Q factor to the refractive index of the surface conductive layer using
57 Equation (1). All the surface of the diamond PhC is supposed to be hydrogenated as confirmed by
58
59
60
61
62
63
64
65

XPS analysis. The real and imaginary part of the refractive index of the SCL can then be calculated as a function of the SCL thickness from the experimentally measured wavelengths shift and Q factors (**Figure 7**).

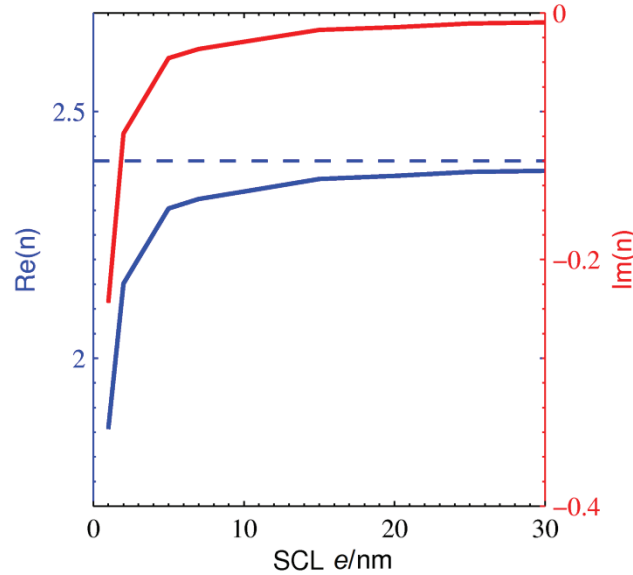


Figure 7. Evolution of the real and imaginary parts of the surface conductive layer of hydrogenated diamond as a function of the thickness of this layer (e).

Because the wavelength shift depends on the volume of the region of modified refractive index probed by the electromagnetic field as seen in Equation (1), its measure only gives us information on the product of the refractive index change by the thickness of the SCL. Nevertheless, for a typical average SCL thickness of 15 nm, the refractive index calculated from the measurements is equal to $2.36 - 0.014i$. As can be seen, the refractive index change is in the order of 2% and even smaller if the SCL spreads over several tens of nanometers. Considering that with a moderate quality factor of 2000, wavelength shifts of the resonance as small as 0.1 nm can be easily observed, refractive index changes of less than 0.1 % that spread over 15 nm in the diamond layer can be detected with this kind of photonic crystal. The imaginary part of the refractive index is equivalent to propagation losses of the order of 1000 cm^{-1} . Even if the thickness of the conductive layer is small, this value can be considered very high in the perspectives of diamond photonic circuits where ultra-high quality factor cavities and low loss waveguide are required. As a consequence, such

1 hydrogenated surfaces may be a limitation for sensing using PhCs as the detection limit would be
2 reduced. Indeed, the conduction phenomenon will still occur on a functionalized surface and, unless
3 the sensing property specifically addresses this surface conductivity property as for diamond-based
4 ion sensitive field effect transistors,^[40] it may be a limitation. However, the geometry used here
5 largely compensates this, and one could expect that it would still be perfectly adapted for real-time
6 detection measurements. Anyway, a full oxidation of the diamond surface, for example using a UV
7 treatment, may thus appear as a prerequisite for the exploitation of diamond photonic devices. As
8 we showed, both stability and efficiency will be higher on oxidized diamond based PhC than on
9 hydrogenated.

3. Conclusion

10 We have investigated the sensitivity of diamond slotted cavities in photonic crystals to chemical
11 surface modifications. We demonstrate that the optical properties of the diamond sPhC are highly
12 affected after simple surface treatments and namely hydrogenation and oxidation. We observed that
13 a resonance wavelength shift of the cavity occurs and is accompanied by a decrease of the Q factor
14 when the surface chemistry is simply turned from oxidized to hydrogenated. Interestingly, this
15 phenomenon is reversible as the initial values of the Q factor are recovered when the surface is re-
16 oxidized. This result can be attributed to an intern phenomenon related to a property of the material,
17 that is the apparition of a conductive layer at the surface when diamond is hydrogenated. This
18 electronic modification of the material strongly modifies the optical features of diamond sPhCs.
19 Since these characteristics are directly depending of the optical environment, the use of diamond
20 slotted PhC is an effective though indirect approach to get an estimate of the refractive index of the
21 surface conductive layer. These experimental results give a strong indication of the sensitivity of
22 slotted PhC cavity in diamond since it can detect the refractive index changes induced by surface
23 chemistry. As a matter of fact, these results are very promising for the realization of very sensitive
24 sensors based on diamond PhC with specific functionalization.

4. Experimental Section.

4.1. Fabrication process

4.1.1 Diamond layer preparation

For this study, we have used nanocrystalline diamond films with a columnar structure exhibiting a thickness of 400 nm deposited on two-inch Si (100) substrates wafers. They were grown at CEALIST using chemical vapor deposition assisted by microwave plasma (MPCVD) with a diamond nanoseeding treatment. The deposition was performed under 35 hPa pressure using methane diluted in hydrogen (0.6% CH₄/H₂) at a total flow of 250 sccm. The microwave power was 1100 W and the substrate was held at a temperature of 1123K. The growth rate was 220 nm/h.^[41] The root mean square (RMS) roughness of the 400-nm thick resulting diamond films is around 10 nm with a peak to valley roughness that can reach 80 nm. This roughness prevents the use of e-beam lithography and the achievement of high quality factor cavities due to the strong scattering at the surface. To smooth the diamond layer, a 200-nm thick hydrogen silsesquioxane (HSQ) layer is first spin-coated on the rough polycrystalline diamond layer and baked on a hot plate. This results in a smooth surface silica-like layer on top of the sample. The layers are then etched using an inductively coupled plasma (ICP) reactive ion etching with oxygen and argon. A 360-nm layer of smooth diamond is finally obtained. Silica residues are removed in hydrofluoric acid. The RMS roughness can reach 1nm only on a 10x10 μm² area, with a peak to valley roughness below 10 nm.

4.1.2 PhC fabrication

The whole fabrication process consists of the following standard steps: a 65-nm thick layer of silicon nitride is first deposited by plasma enhanced chemical vapor deposition (PECVD) on the top of the smoothed diamond layer. Then, e-beam resist is spin-coated on the nitride layer. The photonic crystal and the access waveguide are patterned in the resist using electronic lithography. Using an ICP reactive ion etching (RIE), the pattern is transferred from the resist to nitride and then from nitride to diamond. The remaining nitride mask is removed in hydrofluoric acid. Finally, to fabricate

1 a free-standing diamond membrane the silicon substrate is partially etched using a vapor phase
2 isotropic XeF₂ etching process.
3

4 4.2. Optical characterization

5
6
7 Light from a tunable laser source with a 1-pm resolution (1500–1680 nm, output power 30 μW) is
8 injected and collected into the access waveguide with the use of two polarization maintaining lensed
9 optical fibers with spot diameter of ~2.75 μm. Light from the output of a waveguide is then sent to a
10 polarizer to keep only the TE component of the field (E field parallel to the plane of the PhC) as in
11 ref.^[42]. The transmitted power is recorded with a photodiode and analyzed with an oscilloscope. For
12 cavity measurements, the wavelength sweep on the oscilloscope was limited to the region around
13 the resonance to maximize the resolution.
14
15
16
17
18
19
20
21
22
23

24 Considering that the photonic crystal waveguide acts as a barrier for the cavity mode, and the length
25 of this barrier determines the coupling of the cavity to the ridge access waveguides as well as the
26 loaded quality factor of the cavity, PhC with different parameters are chosen. A PhC cavity with a
27 long barrier is expected to reach the highest Q factor, while a PhC with a short barrier allows a
28 better guidance and transmission of light, which is more advantageous for sensing applications.
29
30
31
32
33
34
35
36

37 4.3. Surface treatments

38
39 Hydrogenation was achieved using a microwave CVD plasma treatment for 30 minutes. Parameters
40 were tuned with a pressure of 40 hPa of H₂. The microwave power was adjusted to 1 kW in order to
41 reach a temperature of 1023 K measured *in situ* using an optical pyrometer (Ircon Modline 3 series
42 3L). Oxidation was achieved by a UV exposure (OSRAM XERADEX) for 2 hours at 250 hPa
43 under air on samples previously hydrogenated. The chemical surface state of the treated samples
44 was characterized by X-ray Photoelectron Spectroscopy. The dimensions and the difficulty to
45 properly evacuate the charges on free diamond membranes such as the PhC prevent from a direct
46 characterization of them by XPS. Therefore, spectroscopic characterizations were performed on
47 reference samples. These samples are extracted from the smoothed diamond layer used for the
48 fabrication of PhC which were thus exposed to the same treatments. The surface chemistry was
49
50
51
52
53
54
55
56
57
58
59
60
61
62
63
64
65

1 monitored with a monochromatized Al Ka anode (1486.6 eV), calibrated versus the Au 4f7/2 peak
2 located at 84.0 eV. Areas of XPS core levels were extracted after a Shirley correction of the
3 background. Carbon and oxygen contents are calculated from XPS spectra after correction by the
4 photoionization cross-sections. A curve fitting procedure was performed to extract the components
5 in the C 1s spectra. Voigt functions were used with a Lorentzian width of 0.4 eV for C 1s.
6
7
8
9
10
11
12
13

14 Acknowledgements

15 C. Blin would like to thank the financial support from the French Atomic Energy Commission. X.
16 Checoury gratefully acknowledges CEA for the support provided for his “Chaire CEA/Université
17 Paris Sud”. This work was also supported by the French RENATECH network and Conseil général
18 de l’Essonne. Authors thank J-C. Arnault for providing facilities and support with XPS recordings.
19
20
21
22
23

24 Received: ((will be filled in by the editorial staff))

25 Revised: ((will be filled in by the editorial staff))

26 Published online: ((will be filled in by the editorial staff))
27
28
29
30
31

32 References

- 33
34 [1] J. Homola, *Chem. Rev.* **2008**, *108*, 462.
35
36 [2] C. a. Barrios, M. J. Bañuls, V. González-Pedro, K. B. Gylfason, B. Sánchez, A. Griol, a.
37 Maqueira, H. Sohlström, M. Holgado, R. Casquel, *Opt. Lett.* **2008**, *33*, 708.
38
39 [3] E. Kuramochi, M. Notomi, S. Mitsugi, A. Shinya, T. Tanabe, T. Watanabe, *Appl.Phys. Lett.*
40 **2006**, *88*.
41
42 [4] B. S. Song, S. Noda, T. Asano, Y. Akahane, *Nat.Mater.***2005**, *4*, 207.
43
44 [5] E. Chow, A. Grot, L. W. Mirkarimi, M. Sigalas, G. Girolami, *Opt. Lett.* **2004**, *29*, 1093.
45
46 [6] M. G. Scullion, A. Di Falco, T. F. Krauss, *Biosensors & bioelectronics* **2011**, *27*, 101.
47
48 [7] a) M. Lee, P. M. Fauchet, *Optics Express* **2007**, *15*, 4530; b) N. Skivesen, A. Têtu, M.
49 Kristensen, J. Kjems, L. H. Frandsen, P. I. Borel, *Optics Express* **2007**, *15*, 3169; c) S. Pal,
50 A. R. Yadav, M. A. Lifson, J. E. Baker, P. M. Fauchet, B. L. Miller, *Biosensors and*
51 *Bioelectronics* **2013**, *44*, 229.
52
53 [8] M. Borselli, T. J. Johnson, O. Painter, *Appl. Phys. Lett.* **2006**, *88*, 131114.
54
55 [9] a) R. C. Major, X.-Y. Zhu, *Langmuir* **2001**, *17*, 5576; b) Z. Lin, T. Strother, W. Cai, X. Cao,
56 L. M. Smith, R. J. Hamers, *Langmuir* **2002**, *18*, 788.
57
58
59
60
61
62
63
64
65

- 1
2
3
4
5
6
7
8
9
10
11
12
13
14
15
16
17
18
19
20
21
22
23
24
25
26
27
28
29
30
31
32
33
34
35
36
37
38
39
40
41
42
43
44
45
46
47
48
49
50
51
52
53
54
55
56
57
58
59
60
61
62
63
64
65
- [10] a) M. Liao, S. Hishita, E. Watanabe, S. Koizumi, Y. Koide, *Adv. Mater. (Deerfield Beach, Fla.)* **2010**, *22*, 5393; b) O. a. Williams, *Diam. and Rel. Mater.* **2011**, *20*, 621; c) M. Dankerl, M. V. Hauf, M. Stutzmann, J. a. Garrido, *Phys. Status Solidi (a)* **2012**, *209*, 1631. d) P. Bergonzo, A. Bongrain, E. Scorsone, A. Bendali, L. Rousseau, G. Lissorgues, P. Mailley, Y. Li, T. Kauffmann, F. Goy, *IRBM* **2011**, *32*, 91;
- [11] I. Aharonovich, A. D. Greentree, S. Praver, *Nat. Photon.* **2011**, *5*, 397.
- [12] A. Faraon, C. Santori, Z. Huang, V. M. Acosta, R. G. Beausoleil, *Phys. Rev. Lett.* **2012**, *109*, 2.
- [13] B. J. M. Hausmann, I. B. Bulu, P. B. Deotare, M. McCutcheon, V. Venkataraman, M. L. Markham, D. J. Twitchen, M. Lončar, *Nano Lett.* **2013**, *13*, 1898.
- [14] X. Checoury, D. Néel, P. Boucaud, C. Gesset, H. Girard, S. Saada, *Appl. Phys. Lett.* **2012**, *171115*, 1.
- [15] a) A. Hartl, E. Schmich, J. A. Garrido, J. Hernando, S. C. R. Catharino, S. Walter, P. Feulner, A. Kromka, D. Steinmuller, M. Stutzmann, *Nat. Mater.* **2004**, *3*, 736; b) B. Sun, S. E. Baker, J. E. Butler, H. Kim, J. N. Russell, L. Shang, K.-Y. Tse, W. Yang, R. J. Hamers, *Diam. and Rel. Mater.* **2007**, *16*, 1608; c) W. Yang, O. Auciello, J. E. Butler, W. Cai, J. A. Carlisle, J. E. Gerbi, D. M. Gruen, T. Knickerbocker, T. L. Lasseter, J. N. Russell, L. M. Smith, R. J. Hamers, *Nat. Mater.* **2002**, *1*, 253.
- [16] a) S. Tomljenovic-Hanic, M. J. Steel, C. M. de Sterke, J. Salzman, *Optics Express* **2006**, *14*, 3556; b) I. Bayn, J. Salzman, *Eur. Phys. J. Appl. Phys.* **2007**, *37*, 19; c) C. Kreuzer, J. Riedrich-Möller, E. Neu, C. Becher, *Opt. Express* **2008**, *16*, 1632; d) S. Tomljenovic-Hanic, A. D. Greentree, C. M. de Sterke, S. Praver, *Opt. Express* **2009**, *17*, 6465; e) T. M. Babinec, J. T. Choy, K. J. M. Smith, M. Khan, M. Loncar, *J. of Vac. Sci. & Tech. B* **2011**, *29*, 10601
- [17] C. F. Wang, R. Hanson, D. D. Awschalom, E. L. Hu, T. Feygelson, J. Yang, J. E. Butler, *Appl. Phys. Lett.* **2007**, *91*, 201112.
- [18] M. P. Hiscocks, C.-H. Su, B. C. Gibson, A. D. Greentree, L. C. L. Hollenberg, F. Ladouceur, *Opt. Express.* **2009**, *17*, 7295.
- [19] T. Yamamoto, M. Notomi, H. Taniyama, E. Kuramochi, Y. Yoshikawa, Y. Torii, T. Kuga, *Opt. Express* **2008**, *16*, 13809.
- [20] a) S.-H. Kwon, T. Sunner, M. Kamp, A. Forchel, *Opt. Express* **2008**, *16*, 11709; b) A. Di Falco, L. O. Faolain, T. F. Krauss, *Appl. Phys. Lett.* **2009**, *063503*, 6; c) J. Jagerska, H. Zhang, Z. Diao, N. Le Thomas, R. Houdré, *Opt. Lett.* **2010**, *35*, 2523.
- [21] I. M. White, X. Fan, *Opt. Express* **2008**, *16*, 1020.